

A topographically forced asymmetry in the martian circulation and climate

Mark I. Richardson* & R. John Wilson†

* Division of Geological and Planetary Sciences, California Institute of Technology, MC 150-21, Pasadena, California 91125, USA

† Geophysical Fluid Dynamics Laboratory, National Oceanic and Atmospheric Administration, PO Box 308, Princeton, New Jersey 08542, USA

Large seasonal and hemispheric asymmetries in the martian climate system are generally ascribed to variations in solar heating associated with orbital eccentricity¹. As the orbital elements slowly change (over a period of $>10^4$ years), characteristics of the climate such as dustiness and the vigour of atmospheric circulation are thought to vary²⁻⁵, as should asymmetries in the climate (for example, the deposition of water ice at the northern versus the southern pole). Such orbitally driven climate change might be responsible for the observed layering in Mars' polar deposits by modulating deposition of dust and water ice^{3,5,6}. Most current theories assume that climate asymmetries completely reverse as the angular distance between equinox and perihelion changes by 180°. Here we describe a major climate mechanism that will not precess in this way. We show that Mars' global north-south elevation difference forces a dominant southern summer Hadley circulation that is independent of perihelion timing. The Hadley circulation, a tropical overturning cell responsible for trade winds, largely controls interhemispheric transport of water and the bulk dustiness of the atmosphere⁷⁻¹¹. The topography therefore imprints a strong handedness on climate, with water ice and the active formation of polar layered deposits more likely in the north.

Models suggest that the meridional circulation on Mars is characterized by a dominant cross-equatorial ('solstitial') Hadley circulation except during a brief transitional period near the equinoxes^{7,8,12,13} (Fig. 1). The circulation has upwelling in the summer tropics, resulting in adiabatic cooling, and downwelling in the winter tropics, which produces adiabatic warming (on Earth, these upwelling and downwelling belts create the cloud and rain characteristic of the equatorial rain forests, and the dry, clear atmosphere over the subtropical deserts). In this way, the dominant Hadley cell transports heat from the summer hemisphere into the winter hemisphere. It is accompanied by a very much weaker cell operating exclusively in the summer hemisphere. The martian mean-meridional circulation is similar to that of the Earth¹⁴⁻¹⁶, although it is more exaggerated owing to the lack of martian oceans to buffer seasonal oscillations in surface temperature. On Mars, however, the solstitial cells are not of equal intensity or extent—the dominant southern summer Hadley cell is roughly twice as intense as that of the northern summer^{7,12}. This is partly due to the planetary eccentricity (0.093) and the fact that perihelion occurs just before the southern summer solstice, resulting in solar incident radiation being as much as 44% higher than experienced in northern summer—southern summer is shorter, but more intense than northern summer.

The influence of the Hadley circulation on climate, through the transport and mixing of dust and water vapour, can be illustrated with output from the Geophysical Fluid Dynamics Laboratory (GFDL) Mars general circulation model (GCM)^{8,11} (Fig. 1). These simulations show that the vertical distribution of dust within the atmosphere is largely determined by the depth of the atmosphere mixed by the Hadley cell. The simulations also illustrate the fact that interhemispheric transport of water is dominated by conveyance in the upper-level Hadley circulation (Fig. 1b). The low-level return flow brings relatively dry air into the summer hemisphere. The

vertical distribution of dust plays an important role in determining the bulk dustiness of the atmosphere^{8,9}, while the nature of the water cycle and the stability of surface water deposits in communication with the atmosphere is critically sensitive to the vigour of interhemispheric water transport^{10,11}. For these reasons, the Hadley circulation is a major factor in the martian climate and is the focus of this study.

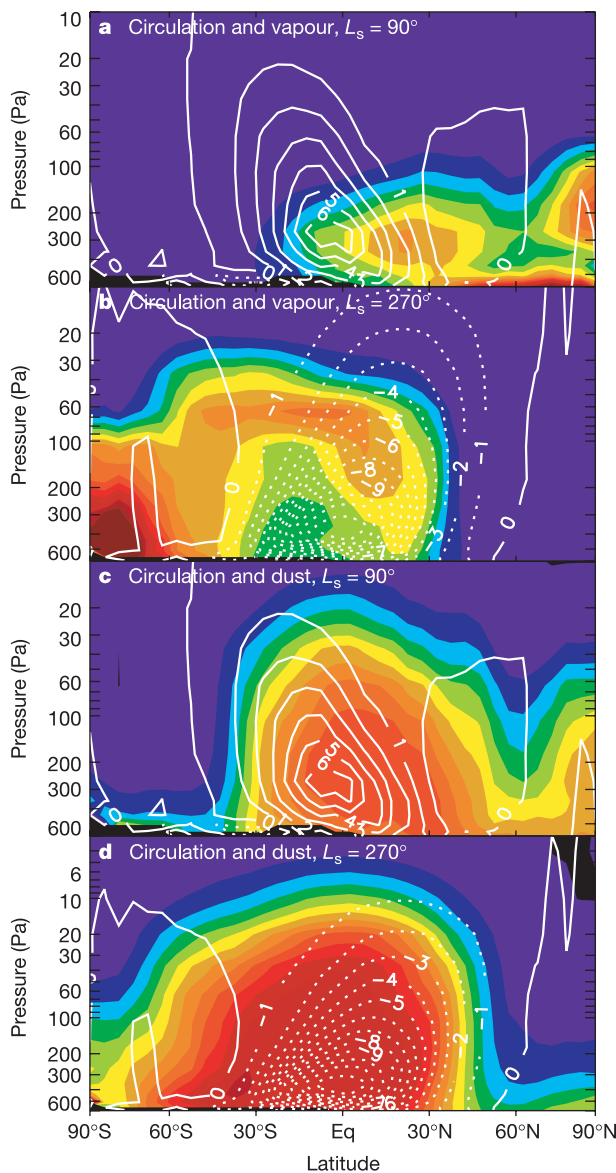


Figure 1 Mars GCM output illustrating the Hadley circulation's strong control of water vapour transport and the global mixing of dust. Zonal-average output are shown for northern summer, $L_s = 90^\circ$, and southern summer, $L_s = 270^\circ$, where L_s is the angular measure of the season, measured in degrees from 0° at northern spring equinox. Stream-function contours are linear in units of 10^8 kg s^{-1} . Panels **a** and **b** show water vapour mass mixing ratio; **c** and **d** show a quantity linearly related to dust mass mixing ratio. Water is supplied only from the summer polar cap, and subsequent evolution depends on transport and atmospheric condensation. Dust injection at the surface is based on stability. Dust and condensed water are subject to gravitational settling. The dust distribution (a significant atmospheric opacity source) is used to calculate radiative heating rates. Water vapour is assumed to be radiatively inactive. The stream function is the conventional eulerian mean constructed from zonal-average mass convergence. Transformed eulerian mean provides a better representation of transport of trace species when eddy heat and momentum transports are large. For the martian tropical atmosphere, the two formulations are essentially identical (compare the vapour distribution and stream function in southern summer).

In the Earth's atmosphere, the seasonally asymmetric Hadley circulations aggregate to yield two roughly equal cells in the annual average (albeit with cells significantly stronger than would be generated by application of annual-average heating¹⁶). Our simulation of the martian meridional circulation demonstrates that this is not true for Mars (Fig. 2a). The annual average of the mean-meridional (mass transport stream function) circulation shows a clear bias in favour of the southern summer cell. This cell is more extensive, and possesses a stream-function maximum more than twice the magnitude of the residual signature of the northern summer solstice, winter hemisphere cell. Further, the southern summer circulation is dominant regardless of the specific scheme used to treat atmospheric dust radiative heating and of whether the seasonal CO₂ cycle is active or not. The peak stream function in the annual average is roughly 25% of the magnitude of the instantaneous peak for the respective cells.

There are two main external factors which could influence the annual average tropical circulation: the eccentricity and the planetary topography. In particular, Mars possesses a significant zonal-average, north-to-south upward slope (this corresponds to an offset between the planetary centre-of-mass and centre-of-figure^{17,18}) and longitudinal asymmetry in topography¹⁸. Whether eccentricity or topography determines the asymmetry is critical. The former factor will change with the orbital elements, introducing climate variability that will also vary with the orbit, consistent with standard theory²⁻⁶. The latter would introduce a climatic asymmetry that is endogenic, emerging from the shape of the planet and not changing with the spin/orbit configuration. To isolate the eccentricity we reran the model with perihelion moved by 180° from its current

occurrence to $L_s = 70^\circ$ (see caption to Fig. 1 for definition of L_s). Figure 2b shows that the annual-average circulation in this case is little changed from that modelled for the present orbital state. Specifically, the tropical circulation remains dominated by the southern summer solstice, winter hemisphere cell, and cell shapes and stream-function magnitudes are not significantly different. The same result holds true for simulations with a circular orbit, and for simulations with no CO₂ or dust cycles. Eccentricity and the timing of perihelion are clearly not the dominant factors in the hemispheric biasing of the tropical circulation.

Speculation that topography might have an effect on the asymmetric strengths of the solstitial Hadley cells has generally focused on hemispheric differences in longitudinal structure^{12,19}. To isolate the influence of the zonal-mean topography, we undertook GCM simulations with the meridionally varying, zonal-mean component of elevation removed from the topography so that only longitudinal variations in topography of potential importance in the generation of waves and eddies remain. For the current timing of perihelion, Fig. 2c shows that without the dichotomy, the annual-average stream function is essentially symmetric about the equator. (Note that there remains some small hemispheric asymmetry in Fig. 2c that disappears if a smooth, thermally uniform surface is used. This slight deviation from hemispheric symmetry is due to the effect of the longitudinal topographic and surface thermal structure on the circulation.) This result also holds for non-dichotomy simulations run with perihelion at $L_s = 70^\circ$. We note that the dichotomy-free, northern hemisphere cell is significantly weaker in the annual average (by a factor of two in peak stream function) than in the case with real martian topography. The peak stream function for the

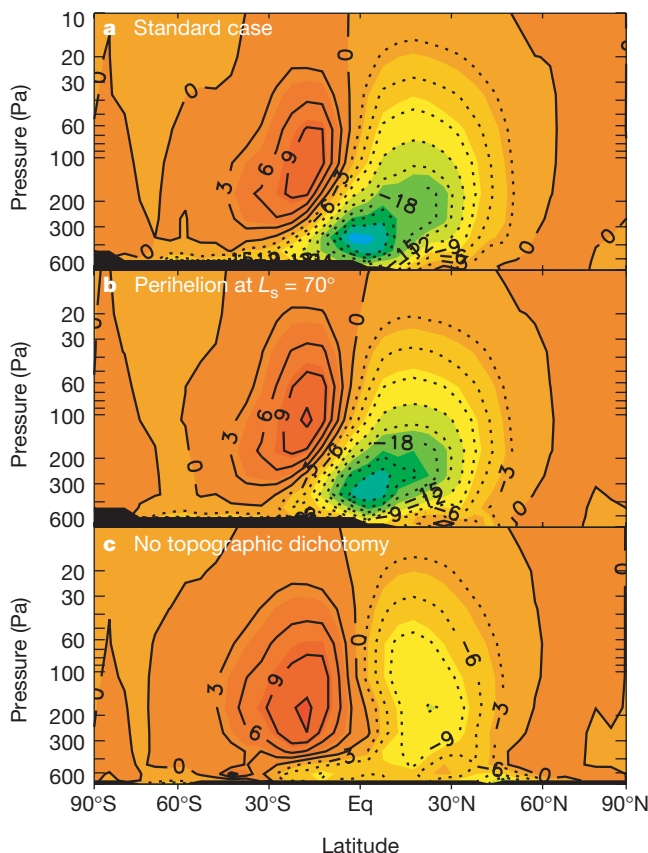


Figure 2 Mars GCM output demonstrating the annual-average bias in the tropical circulation, and that this bias is related to topography rather than the eccentric orbit of the planet. **a, b, c**, Annual-average, zonal-mean meridional stream functions are shown for **a**, observed topography and current orbital properties, **b**, observed topography, but the passage of perihelion moved to $L_s = 70^\circ$, and **c**, dichotomy-free topography, but current orbital properties. The stream functions are displayed in units of 10^8 kg s^{-1} , with positive

values indicating anticlockwise flow in the plane of the page. As in Fig. 1, the stream functions are the conventional eulerian mean. In these panels, the residual signature of the southern summer circulation is captured by the cell extending deep into the northern hemisphere, while the northern summer cell extends into the southern hemisphere. In each case, the dominant solstitial Hadley cell is the one that extends from the summer hemisphere into the winter hemisphere.

southern hemisphere cell is relatively unaffected by the change in topography. Simulations run with zonal-mean topography (not shown) result in a hemispheric bias in cell strength, as with the standard simulation.

These results demonstrate that the annual-average circulation is fundamentally biased by the zonal-mean topographic dichotomy on Mars. Elucidation of the specific mechanism(s) by which this asymmetry comes about requires further study, but probably involves the effect of the higher, southern hemisphere acting as an elevated heat source, and the effect of the cross-equatorial slope as a dynamical impediment to northern summer Hadley return flow. The former effect results from the fact that surface temperatures decrease much more slowly with pressure than do air temperatures. Thus elevated ground can significantly influence meridional gradients of temperature on pressure surfaces well above the ground, leading to biases in forcing of the tropical circulation, in analogy to the effect of the Tibetan plateau on the Indian monsoon²⁰.

The Hadley circulation has a strong influence on the cycles of dust and water, as described above. However, the evolution of water and dust within the climate system probably depends on a number of factors. For transport of water, the mixing capacity of the atmosphere must be convolved with the seasonal exchange of vapour with the seasonal and residual water ice caps. Water can also condense in the atmosphere at a level depending on the atmospheric temperature structure. If this level is sufficiently low, condensation will impede cross-equatorial transport^{21,22}. For dust mixing, the physics of dust injection at the surface is of major importance, and will depend on surface wind stresses and the temperature contrast between the surface and atmosphere across the boundary layer. Because dust is a radiatively active species there exists an important feedback between dust distribution, the distribution of radiative heating, and the circulation, with the circulation largely determining the dust distribution. Further, it is possible that the dust distribution is also influenced by the water cycle, through the use of dust particles as water cloud condensation nuclei.

Despite the complexity of the martian climate system, we can state that the asymmetry imposed on the climate by the topographic biasing of the Hadley circulation will have a uniquely important influence. Unlike the myriad other mechanisms operating within the system, which are determined by spatial patterns of solar heating, the topographic biasing of the Hadley circulation will impose a handedness upon the climate system that will remain as a residual when averaged over integer combinations of precessional cycles. While topography may also influence the CO₂ cycle on Mars²⁶, affecting the water cycle by varying the fraction of the year that water ice caps are exposed, the biasing of the circulation is far more direct and less susceptible to compensation by other processes (topographic biasing of the current CO₂ cycle would predict a permanent cap at the north—in reality, it is at the south). As such, this bias in the climate system is of great importance and requires further quantitative analysis.

We now consider how, and on what timescales, the topographic biasing will influence climate. The primary impact of the bias on the water cycle results from the net annual-average transport from the southern to northern hemispheres. Simulations using current orbital parameters, but with exposed water-ice caps prescribed at both poles, show that a southern residual water-ice cap is dynamically unstable with respect to the northern cap, even when cap temperatures are constrained to give no thermodynamic advantage to the north¹¹. It is possible that at high obliquity and with perihelion in northern summer, the northern cap will become unstable with respect to a southern residual water cap. However, it is equally clear that the net south-to-north transport generated by the dichotomy dictates that there will be more orbital configurations in which the northern cap, rather than the southern cap, will be stable.

Indeed, the existence of a southern residual water-ice cap may

require special combinations of eccentricity, obliquity and argument of perihelion. Asynchronous variation of these parameters (periods of 2 Myr, 0.12 Myr and 0.17 Myr, respectively²³) may imply that a southern water-ice cap occurs with a period of >10⁶ years rather than the ~10⁵ years predicted if one considers only cyclic variation in solar heating driven by precession. Polar layered deposit formation is poorly understood⁶, but it is widely held that layering develops at times of enhanced polar deposition of dust and water ice^{3–6}. If a residual water-ice cap is an important agent of layered deposit formation, then the tendency for water ice to be preferentially stable at the northern pole, and hence for a water ice cap to be much more likely to occur, suggests that the northern layered deposits should be more frequently active than those at the south, potentially by an order of magnitude or so. Clearly, the relationship between the topographic biasing of the water cycle and the disparate age of the layered deposits (with the south known to be much older than the north)²⁴ should be investigated in more detail.

Dark layers in the deposits are commonly ascribed to deposition during dustier climatic periods^{5,6}. The instantaneous strength of the Hadley circulation will play a large role in the bulk dustiness of the atmosphere by vertically and meridionally spreading dust. Models also suggest strong increases in surface winds as the Hadley cell intensifies^{7–9,12,13,25}, and these winds may contribute to lofting of dust, increasing the surface injection rate.

Although there are many configurations in which the northern summer solstitial Hadley cell may be dominant, the topographic bias dictates that the southern summer cell is more likely to be dominant, averaged over the cycles of precession, obliquity and eccentricity. As such, not only is it more likely that water ice will be stable at the northern pole and consequently that polar layered terrain formation is more common there, but the likelihood of southern summer being dustier than northern summer suggests that a ready supply of dust will be available to form layers. □

Received 9 October 2001; accepted 28 January 2002.

- Zurek, R. W. *et al.* in *Mars* (eds Kieffer, H. H., Jakosky, B. M., Snyder, C. W. & Matthews, M. S.) 835–933 (Univ. Arizona Press, Tucson, 1992).
- Ward, W. R. Climatic variations on Mars. I. Astronomical theory of insolation. *J. Geophys. Res.* **97**, 3375–3386 (1974).
- Murray, B. C., Ward, W. R. & Yeung, S. C. Periodic insolation variations on Mars. *Science* **180**, 638–640 (1973).
- Kieffer, H. H. & Zent, A. P. in *Mars* (eds Kieffer, H. H., Jakosky, B. M., Snyder, C. W. & Matthews, M. S.) 1180–1220 (Univ. Arizona Press, Tucson, 1992).
- Toon, O. B., Pollack, J. B., Ward, W., Burns, J. A. & Bilski, K. The astronomical theory of climate change on Mars. *Icarus* **44**, 552–607 (1980).
- Thomas, P., Squyres, S. W., Herkenhoff, K., Howard, A. & Murray, B. in *Mars* (eds Kieffer, H. H., Jakosky, B. M., Snyder, C. W. & Matthews, M. S.) 767–798 (Univ. Arizona Press, Tucson, 1992).
- Haberle, R. M., Leovy, C. B. & Pollack, J. B. Some effects of global dust storms on the atmospheric circulation of Mars. *Icarus* **50**, 322–367 (1982).
- Wilson, R. J. & Hamilton, K. Comprehensive model simulation of thermal tide in the Martian atmosphere. *J. Atmos. Sci.* **53**, 1290–1326 (1996).
- Murphy, J. R. *et al.* Three-dimensional numerical simulation of Martian global dust storms. *J. Geophys. Res.* **100**, 26357–26376 (1995).
- Houben, H., Haberle, R. M., Young, R. E. & Zent, A. P. Modeling the Martian seasonal water cycle. *J. Geophys. Res.* **102**, 9069–9083 (1997).
- Richardson, M. I. & Wilson, R. J. Investigation of the nature and stability of the Martian seasonal water cycle with a general circulation model. *J. Geophys. Res.* (in the press).
- Haberle, R. M. *et al.* Mars atmospheric dynamics as simulated by the NASA Ames general-circulation model. 1. The zonal-mean circulation. *J. Geophys. Res.* **98**, 3093–3123 (1993).
- Forget, F. *et al.* Improved general circulation models of the Martian atmosphere from the surface to above 80 km. *J. Geophys. Res.* **104**, 24155–24175 (1999).
- Oort, A. H. & Rasmussen, E. M. On the annual variation of the monthly mean meridional circulation. *Mon. Weath. Rev.* **98**, 423–442 (1970).
- Peixoto, J. P. & Oort, A. H. *Physics of Climate* (American Institute of Physics, New York, 1992).
- Lindzen, R. S. & Hou, A. Y. Hadley circulation for zonally averaged heating centered off the equator. *J. Atmos. Sci.* **45**, 2416–2427 (1988).
- Smith, D. E. & Zuber, M. T. The shape of Mars and the topographic signature of the hemispheric dichotomy. *Science* **271**, 184–188 (1996).
- Smith, D. E. *et al.* The global topography of Mars and implications for surface evolution. *Science* **284**, 1495–1503 (1999).
- Haberle, R. M. *et al.* Mars general circulation model simulations with MOLA topography. *Icarus* (submitted).
- Molnar, P. & Emanuel, K. A. Temperature profiles in radiative-convective equilibrium above surfaces at different heights. *J. Geophys. Res.* **104**, 24265–24271 (1999).
- Clancy, R. T. *et al.* Water vapor saturation at low altitudes around Mars aphelion: A key to Mars climate? *Icarus* **122**, 36–62 (1996).

22. Richardson, M. I., Wilson, R. J. & Rodin, A. V. Water ice clouds in the Martian atmosphere: General circulation model experiments with a simple cloud scheme. *J. Geophys. Res.* (submitted).
23. Ward, W. R. in *Mars* (eds Kieffer, H. H., Jakosky, B. M., Snyder, C. W. & Matthews, M. S.) 298–320 (Univ. Arizona Press, Tucson, 1992).
24. Herkenhoff, K. E. & Plaut, J. J. Surface ages and resurfacing rates of the polar layered deposits on Mars. *Icarus* **144**, 243–253 (2000).
25. Fenton, L. K. & Richardson, M. I. Martian surface winds: Insensitivity to orbital changes and implications for aeolian processes. *J. Geophys. Res.* **106**, 32885–32902 (2001).
26. Jakosky, B. M., Henderson, B. G. & Mellon, M. T. The Mars water cycle at other epochs—Recent history of the polar caps and layered terrain. *Icarus* **102**, 286–297 (1993).

Acknowledgements

Discussions were provided by K. Emanuel, I. Held, A. Ingersoll, T. Schneider, and Y. Yung. We thank P. Gierasch for comments on the manuscript.

Competing interests statement

The authors declare that they have no competing financial interests.

Correspondence and requests for materials should be addressed to M.I.R. (e-mail: mir@gps.caltech.edu).

Ferromagnetism in one-dimensional monatomic metal chains

P. Gambardella[†], A. Dallmeyer[†], K. Maiti[†], M. C. Malagoli[†], W. Eberhardt^{†‡}, K. Kern^{*§} & C. Carbone^{†||}

^{*} Institut de Physique des Nanostructures, EPF-Lausanne, CH-1015 Lausanne, Switzerland

[†] Institut für Festkörperforschung, Forschungszentrum Jülich, D-52425 Jülich, Germany

[‡] Berliner Elektronenspeicherring-Gesellschaft für Synchrotronstrahlung m.b.H., Albert-Einstein-Straße 15, 12489 Berlin, Germany

[§] Max-Planck-Institut für Festkörperforschung, Heisenbergstr. 1, D-70569 Stuttgart, Germany

^{||} Istituto di Struttura della Materia, Consiglio Nazionale delle Ricerche, Area Science Park, I-34012 Trieste, Italy

Two-dimensional systems, such as ultrathin epitaxial films and superlattices, display magnetic properties distinct from bulk materials¹. A challenging aim of current research in magnetism is to explore structures of still lower dimensionality^{2–6}. As the dimensionality of a physical system is reduced, magnetic ordering tends to decrease as fluctuations become relatively more important⁷. Spin lattice models predict that an infinite one-dimensional linear chain with short-range magnetic interactions spontaneously breaks up into segments with different orientation of the magnetization, thereby prohibiting long-range ferromagnetic order at a finite temperature^{7–9}. These models, however, do not take into account kinetic barriers to reaching equilibrium or interactions with the substrates that support the one-dimensional nanostructures. Here we demonstrate the existence of both short- and long-range ferromagnetic order for one-dimensional monatomic chains of Co constructed on a Pt substrate. We find evidence that the monatomic chains consist of thermally fluctuating segments of ferromagnetically coupled atoms which, below a threshold temperature, evolve into a ferromagnetic long-range-ordered state owing to the presence of anisotropy barriers. The Co chains are characterized by large localized orbital moments and correspondingly large magnetic anisotropy energies compared to two-dimensional films and bulk Co.

Since the work of Ising⁸, magnetism in one-dimensional (1D) systems has been the subject of continuous theoretical^{4,5,7–10} and experimental^{2,6,11} research. Progress in atomic engineering makes it possible today to build 1D arrays of transition-metal chains by self-

assembly epitaxial techniques on suitable substrates^{12,13}. Pioneering experiments^{14–16} in this direction investigated the magnetic behaviour of Fe stripes 1–10 nm wide obtained by step-flow growth on W(110) and Cu(111) surfaces. Ideally, one would like to construct monatomic chains in very large numbers while maintaining a fine control on the dimensions, uniformity and spatial distribution of the individual chains. We have shown¹⁷ that it is possible to produce high-density ($5 \times 10^6 \text{ cm}^{-1}$) arrays of parallel monatomic chains with unprecedented uniformity and even spacing by growing Co on a high-quality Pt vicinal surface in a narrow (250–300 K) temperature range. The scanning tunnelling microscopy (STM) images in Fig. 1 illustrate the regular step structure of the vicinal Pt(997) surface (Fig. 1a) and the fabrication of monatomic Co wires by decoration of the steps (Fig. 1b)¹⁷.

The magnetism of the Co wires has been investigated by X-ray magnetic circular dichroism¹⁸ (XMCD) at beamline ID-12B of the European Synchrotron Radiation Facility in Grenoble. Representative results for the circular dichroism in X-ray absorption spectroscopy (XAS) at the Co L_{2,3} absorption edges for the monatomic wires are shown in Fig. 2a and compared with one monolayer (Fig. 2b) and bulk Co spectra (Fig. 2c). The difference between the two spectra for left- and right-handed polarization, reported in the lower panel, shows that the wires are characterized by a strong dichroism that results from the alignment of the Co magnetic moments in an external field of 7 T at 10 K. The amplitude of the dichroic signal is a measure of the magnetization of the Co wire array and contains information on the local character of the atomic moments.

The reduced atomic coordination of the monatomic chains compared to bulk Co and two-dimensional (2D) films has remarkable consequences for the relative size of the local orbital (m_L) and spin (m_S) magnetic moments. Both m_L and m_S are expected to increase as the atomic coordination is reduced in passing from the bulk to the monatomic chains. Local spin density calculations for Co/Pt(997) show that the narrowing of the Co 3d band and the

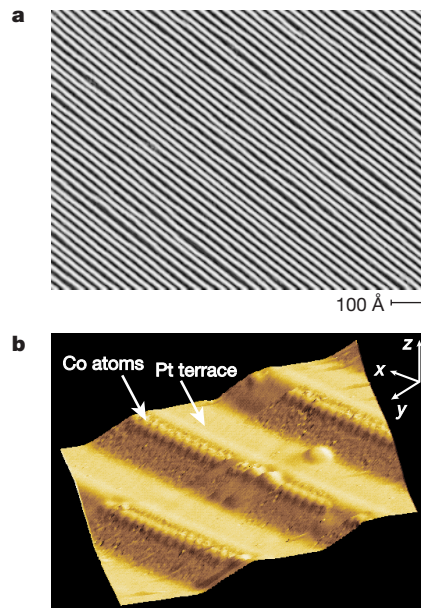


Figure 1 STM topographs of the Pt(997) surface. **a**, Periodic step structure (each white line represents a single step). The surface has a 6.45° miscut angle relative to the (111) direction; repulsive step interactions result in a narrow terrace width distribution centred at 20.2 Å with 2.9 Å standard deviation. **b**, Co monatomic chains decorating the Pt step edges (the vertical dimension is enhanced for better contrast). The monatomic chains are obtained by evaporating 0.13 monolayers of Co onto the substrate held at $T = 260 \text{ K}$ and previously cleaned by ion sputtering and annealing cycles in ultrahigh vacuum (UHV). The chains are linearly aligned and have a spacing equal to the terrace width.